Med Sci Monit, 2000; 6(1): 158-167

Biomechanics of soft tissues

Karol Miller

Department of Mechanical and Materials Engineering, University of Western Australia, Nedlands/Perth, Australia
Sources of financial support: Australian Research Council, Japanese Science and Technology Agency

key words: brain, liver, kidney, mechanical properties, mathematical modelling

SUMMARY

Recent developments in Computer–Integrated and Robot–Aided Surgery (in particular, the emergence of automatic surgical tools and robots (as well as advances in Virtual Reality techniques, call for closer examination of the mechanical properties of very soft tissues (such as brain, liver, kidney, etc.). Moreover, internal organs are very susceptible to trauma. In order to protect them properly against car crash and other impact consequences we need to be able to predict the organ deformation. Such prediction can be achieved by proper mathematical modelling followed by a computer simulation. The ultimate goal of our research into the biomechanics of these tissues is development of corresponding, realistic mathematical models. This paper contains experimental results of in vitro, uniaxial, unconfined compression of swine brain tissue obtained by the author in Mechanical Engineering Laboratory, Japan, and discusses liver and kidney in vivo compression experiments conducted in Highway Safety Research Institute and the Medical Centre of The University of Michigan. The stress–strain curves for investigated tissues are concave upward for all compression rates containing no linear portion from which a meaningful elastic modulus might be determined. The tissue response stiffened as the loading speed increased, indicating a strong stress (strain rate dependence. As the step in the direction towards realistic computer simulation of injuries and surgical procedures, this paper presents two mathematical representations of brain, liver and kidney tissue stiffness. Biphasic and single-phase models are discussed. The biphasic model is shown to be inappropriate due to its inability to account for strong stress-strain relationship. Agreement between the proposed single-phase models and experiment is good for compression levels reaching 30% and for loading velocities varying over five orders of magnitude.

Presented mathematical models can find applications in computer and robot assisted surgery, e. g. the realistic simulation of surgical procedures (including virtual reality), control systems of surgical robots, and non-rigid registration, as well as ergonomic design for injury prevention

INTRODUCTION

Mechanical properties of living tissues form a central subject in Biomechanics. In particular, the properties of the muscular–skeletal system, skin, lungs, blood and blood vessels have attracted much attention, for examples, see [1–5] and references cited therein. The properties of 'very' soft tissues, which do not bear mechanical loads (such as brain, liver and kidney), have not been so thoroughly investigated.

However, recent developments in robotics technology, especially the emergence of automatic surgical tools and robots [6] as well as advances in virtual reality techniques [7], call for closer examination of the mechanical properties of these tissues. Mathematical models of soft tissue mechanical properties may find applications, for example, in a surgical robot control system, where the prediction of deformation is needed [8,9], surgical operation planning and surgeon training systems based on the virtual reality techniques ([7] and references cited

Received: 2000.01.14
Accepted: 2000.02.10
Correspondence address: Karol Miller, Department of Mechanical and Materials Engineering, University of Western Australia, Nedlands/Perth WA 6907, Australia, email: kmiller@mech.uwa.edu.au

therein), where *force feedback* is needed, and *registration* [10], where knowledge of local deformation is required. Such systems for rigid tissues (see e.g. Journal of Computer Aided Surgery) already exist. Their development for 'very' soft tissues is very much dependent on the knowledge of these tissues' mechanical properties and the existence of the appropriate mathematical models. Such models can also help to identify modes of injury, and improve injury prevention techniques [11].

The reported experimental data on the mechanical properties of brain tissue are limited. Ommaya [12] described mammalian brain as a 'soft, yielding structure, not as stiff as a gel nor as plastic as a paste'. Walsh and Schettini [13] and Sahay et al. [14] tried to establish elastic parameters of brain tissues by measuring induced changes in intra-cranial pressure. The experimental data, which might be used to determine mechanical properties of brain tissue, was reported in [15] and [16]. The objective of those papers was providing data for head injury modelling (for discussion see [17]), so that the investigated strain rates (loading velocities) were much higher than those relevant for neurosurgical operation modelling. Based on these experimental results, Pamidi and Advani [18], and Mendis et al. [19] proposed non–linear constitutive relations for human brain tissue. Recently, Guillaume et al. [20] discussed brain response to hypergravity and Donnelly and Medige [21] investigated human brain tissue properties in shear.

Another factor demanding closer examination of the mechanical properties of soft tissues is the increasing requirement for automotive safety. The accurate tissue models are the perquisites for realistic injury simulation and designing methods for injury prevention. Unfortunately, most of the papers discussing types of injuries did so without direct reference to the mechanics of the organs (e.g. [11,22–26]). Some experimental data can be extracted from [27] but, unfortunately, the crucial information about strain rates (loading velocities) applied is not provided in this otherwise helpful book. Recently Farshad et al [28] presented *in vitro* experimental results and a mathematical model of a pig kidney. Schmidlin et al [29] proposed a two dimensional finite element model of the kidney to investigate injury mechanisms in renal trauma. However, a very simple hyperelastic constitutive equation (based on [27]) for the tissue was assumed in that paper. As a result, important velocity dependent phenomena (see e.g. 'Viscous criterion' [30–32]) could not be accounted for.

The theoretical results of this paper are based on the results of *in vivo* experiments on Rhesus monkeys (liver and kidney, [33]), and *in vitro* experiments on swine brains. We attempt to prove that currently popular biphasic model is not appropriate for modelling soft tissue due to its inability to account for strong stress – strain rate dependence. We also show, that a single-phase mathematical model developed here, based on the concept of strain energy function with time dependent material coefficients, is suitable for description of brain, liver and kidney tissue deformation behaviour under compression, at high and medium strain rates, typical for impact loading and surgical procedures.

STRESS-STRAIN RELATIONSHIP FOR BRAIN, LIVER AND KIDNEY

Unconfined compression experiment for swine brain tissue

Specimen preparation

Twelve brains from six–month old swines were collected from a slaughter house. Pigs were terminated according to standard slaughtering procedure and the samples were taken as a by–product. Specimens were not frozen at any time during the procedure. Brain weights ranged between 92.5 and 101.5 grams, close to the weight of a healthy adult swine [34]. After being removed from the dura, each brain was stored in physiological solution at 5°C. Usually, transportation of brains and sample preparation took eleven hours before experiments could begin.

Cylindrical samples of diameter ~30 mm and height ~13 mm were cut. Steel pipe (30 mm diameter) with sharp edges was used to cut the samples. The faces of the cylindrical brain specimens were smoothed manually, using a surgical scalpel. Four samples were taken from the frontal and posterial portions of the Sylvian fissure of each hemisphere for each swine brain. The ventricle surface and the arachnoid membrane formed the top and bottom faces of the sample cylinder. Thus the arachnoid membrane and the structure of the sulci remained as parts of each specimen.

Brain tissue is very soft and adheres upon contacting almost any material. Consequently, it was very difficult to obtain an exact cylindrical shape. Usually, the diameters of opposite faces of the sample differed by approximately 3–4 mm.

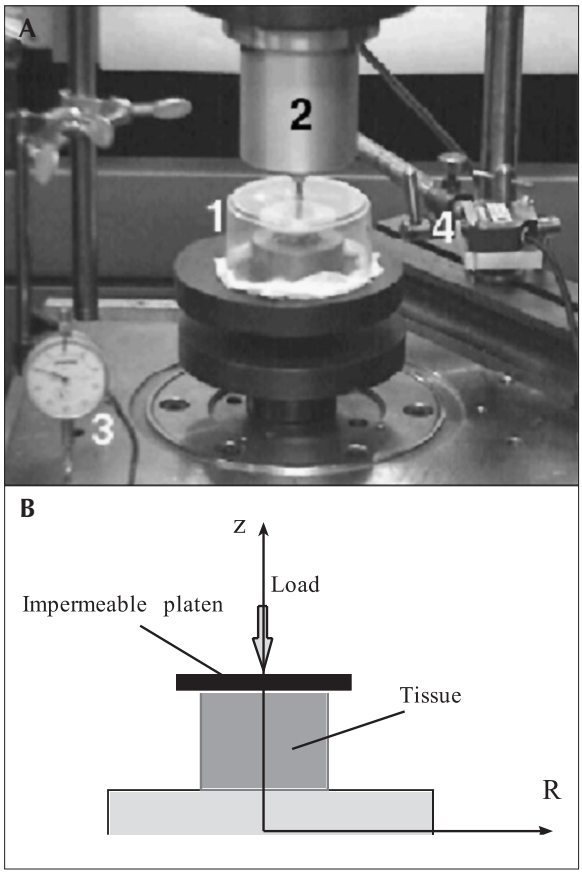

Figure 1. Experiment setting for brain tissue compression.
a) general view with components:
1 – brain tissue specimen and the loading platens,
2 – load cell to measure axial force,
3 – micrometer to measure axial displacement,
4 – laser to measure radial displacement.
b) layout with coordinate axes

Experimental setting and protocol

Uniaxial unconfined compression of swine brain tissue was performed in a testing stand shown in Figure 1. This particular geometry was dictated by the simplifying assumptions, underlying the development of the analytical solution for stresses (see Section 3), used to analyse the experimental data.

The main testing apparatus was a UTM-10T (Orientec Co.) tensile stress machine. Its load cell allowed measurement of compressive force in the range 0.5–9.0 N for loading velocities between 0.005 to 500 mm/min. The vertical displacement (along z-axis in Fig. 1b) was measured by a micrometer with electric analog output. An important part of the experiment was the measurement of the radial displacement by a laser distance meter LB-02/LB-62 (Keyence Corp.). This measurement was intended for determining the level of tissue compressibility as well as the beginning of the loading phase of the experiment. The experiment was documented by automatically taking CCD camera images. The images were used to ensure that during the loading phase samples had uniformly expanded in radial direction as well as that upper or lower faces of the specimen had not sticked to the moving platen or support.

Cylindrical samples of tissue were axially compressed between two impermeable platens. As a result of brain tissue delicacy and adhesiveness, no pre–conditioning was performed. Only one loading cycle was executed on each sample.

To diminish the effects of friction between platens and a sample, polytetrafluoroethylene (PTFE) sheets were attached to the surfaces of the supporting base and movable platen. During overnight tests, to avoid drying of the specimen, the sample was surrounded by wet lignin and covered by a plastic shield. The tests were performed at room temperature (~22°C). At the end of the procedure no signs of dehydration were observed.

The movement of the platen began about one millimetre above the sample. Care was taken to avoid touching the specimen by the platen before starting compression as the sample tended to adhere to the platen and change shape. The start of the loading phase was indicated by the first non–zero reading of the radial displacement by laser distance meter. This method appears to be more reliable than previously used first non–zero readings of the force sensor [15] because the forces at low compression levels are very small. The end of the loading phase was indicated by the point of equalising of the reading of the micrometer measuring the vertical displacement.

RESULTS

In the paper only the results obtained for the loading phase are discussed. The measurements for the following three loading velocities are presented:

- fast: 500 mm min^{-1} (the fastest loading speed possible with our equipment (corresponding to the strain rate of about 0.64 s^{-1},
- medium: 5 mm min^{-1}, corresponding to the strain rate of about $0.64\times10^{-2}s^{-1}$, and
- slow: 0.005 mm min^{-1}, corresponding to the strain rate of about $0.64\times10^{-5}s^{-1}$.

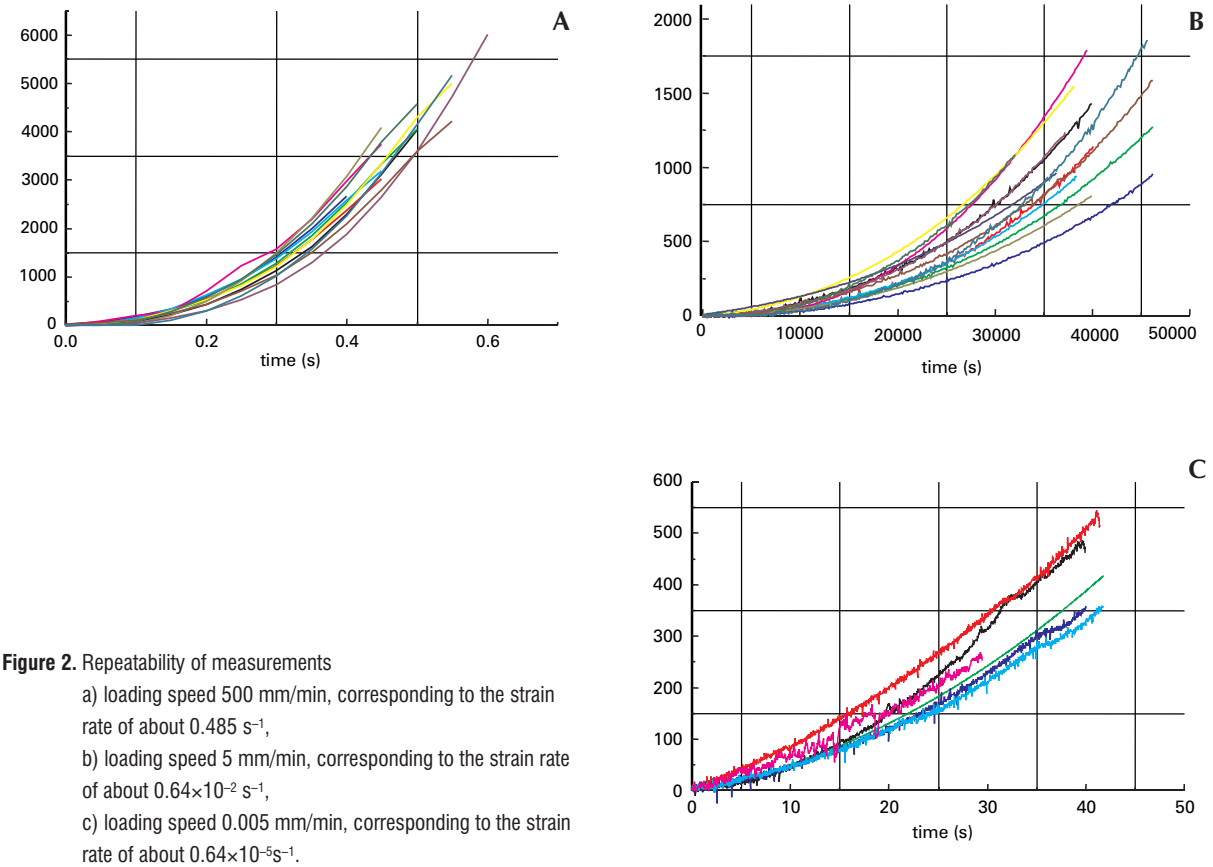

Figure 2. Repeatability of measurements
a) loading speed 500 mm/min, corresponding to the strain rate of about 0.485 s^{-1},
b) loading speed 5 mm/min, corresponding to the strain rate of about 0.64×10^{-2} s^{-1},
c) loading speed 0.005 mm/min, corresponding to the strain rate of about $0.64\times10^{-5}s^{-1}$.

In each test the moving platen stopped after compressing the specimen by about 4.5 mm. Twelve fast, 13 medium speed and 6 slow tests were performed. Each sample was tested once only. The number of slow tests was limited because after each tissue delivery (usually 2 brains) only one overnight test could be performed.

To assess the repeatability of measurements, the Lagrange stresses (vertical force divided by initial cross–section area) versus time for each loading velocity are presented in Figure 2. The coefficient of variation (standard deviation divided by the mean) for slow and medium speed tests was approximately constant and equal to 0.2 and 0.3 respectively. The coefficient of variation for fast test varied between 0.18 and 0.29. These values are significantly lower than 0.5 (the value estimated from Figures 3–6 in [15] (suggesting that the repeatability of experiments is significantly better than that obtained by previous researchers. The results are affected by variations between tissue samples taken from 12 swines, inherent for biological materials, and errors in estimation of sample cross–section area, due to deviations from cylindrical shape (up to 4%). The errors of force and displacement measurements are insignificant (not more than 0.1% of maximum force and displacement).

Figure 3 shows the relationship between the Lagrange stress and true strain ($e = \ln l_z$, where l_z is a stretch in vertical direction, Fig. 1b) for three loading velocities. The standard deviation of the measurements and the theoretical predictions are indicated. The stress-strain curves are concave upward for all compression rates containing no linear portion from which a meaningful elastic modulus could be determined. The tissue response stiffened with the increasing loading speed, indicating a strong stress-strain rate dependence. The results shown in Figure 3 are in general agreement with those published in [15]. The results obtained for $\dot{\lambda}=0.64$ 1/s are very close to those reported in [15], for $\dot{\lambda}=0.8$ 1/s . It needs to be pointed out here, that for slower strain rates there is no other data available for comparisons.

The measurement of the radial displacement was not successful due to the laser distance meter sensitivity to the reflection angle and sample colour changes. The repeatability was not sufficient to state with confidence the value of the finite defor-

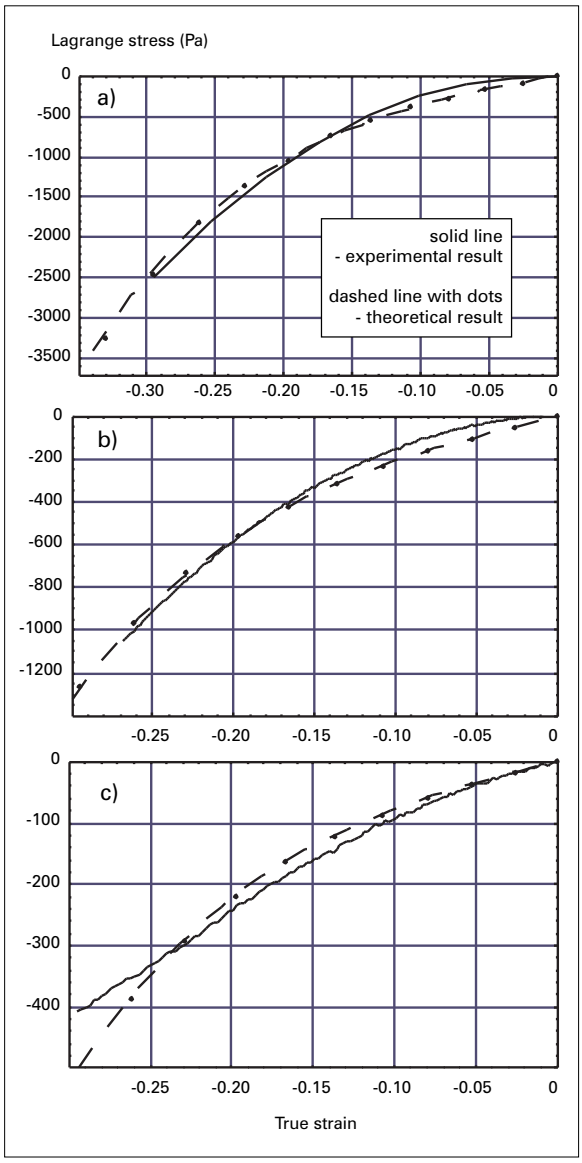

Figure 3. Lagrange stress – true strain relations for swine brain tissue. Experimental versus theoretical results.
a) loading speed 500 mm/min, corresponding to the strain rate of about 0.64 s^{-1},
b) loading speed 5 mm/min, corresponding to the strain rate of about 0.64×10^{-2} s^{-1},
c) loading speed 0.005 mm/min, corresponding to the strain rate of about $0.64\times10^{-5}s^{-1}$.

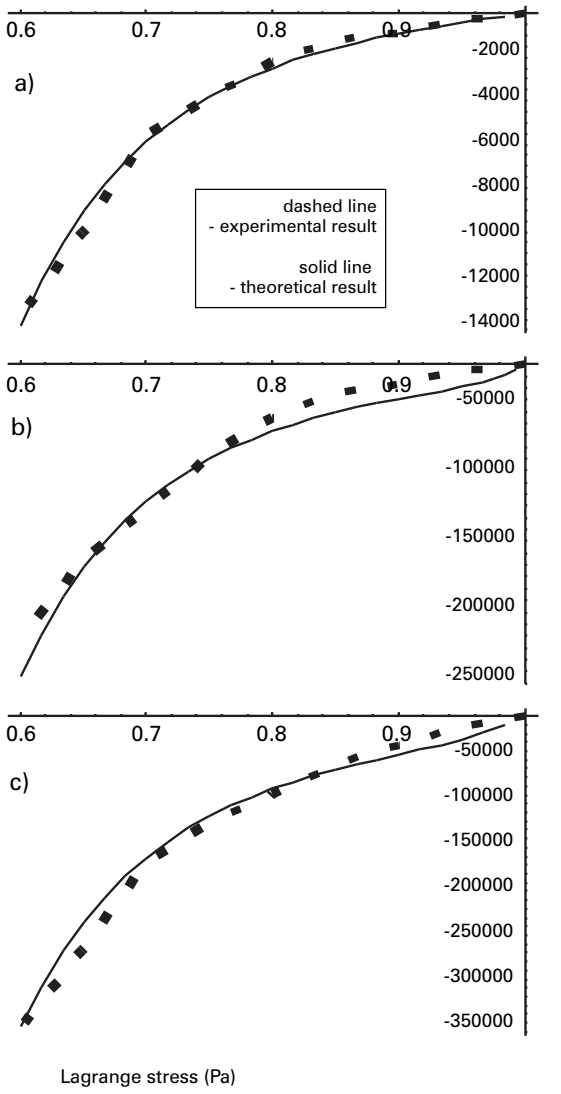

Figure 4. Lagrange stress – elongation (l) relations for Rhesus monkey liver tissue, experimental and theoretical results.
a) loading speed 5 cm/s, corresponding to the strain rate of about 0.225 s^{-1},
b) loading speed 250 cm/s, corresponding to the strain rate of about 11.25 s^{-1},
c) loading speed 500 cm/s, corresponding to the strain rate of about 22.50 s^{-1}.

mation analog of the Poison's ratio of swine brain tissue. As it was not possible to challenge the common assumption of tissue incompressibility (e.g. [15,17–19,35]), in the theoretical part of the paper, the incompressibility of bran tissue is assumed. The laser distance meter was still very useful in determination of the beginning of sample lateral expansion, which was considered as the start of the loading phase.

Unconfined compression of liver and kidney

Melvin et al [33] conducted *in vivo* constant velocity compression tests on livers and kidneys of anaesthetised Rhesus monkeys. The experiments where designed so that the injury mechanisms could be observed. From the perspective of this study, the most valuable results are the stress-strain curves obtained for various loading velocities (Figures 4

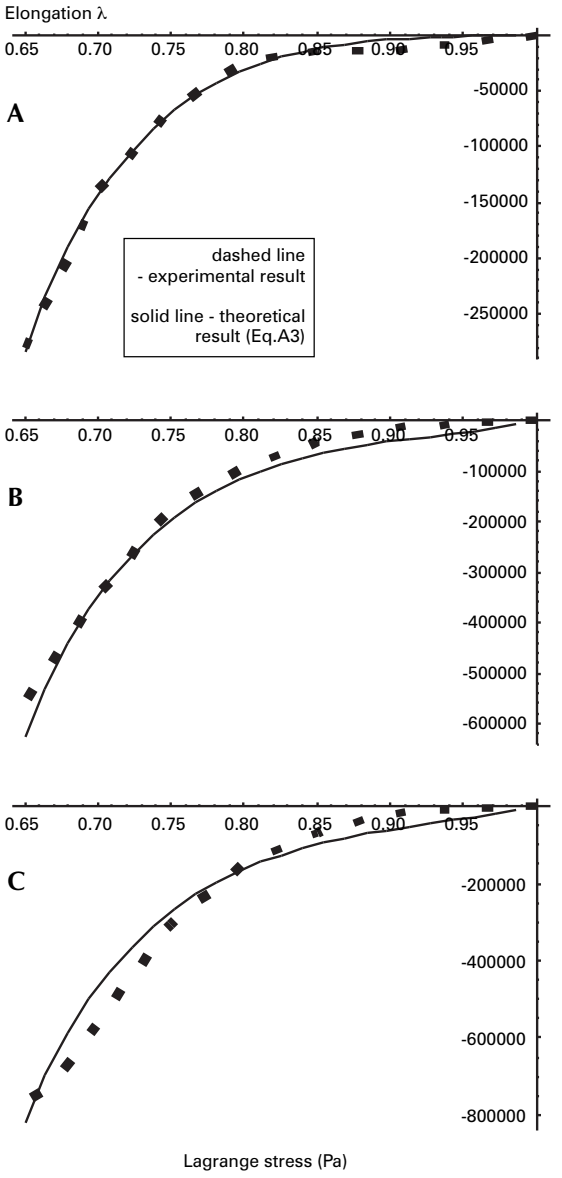

Figure 5. Lagrange stress – elongation (l) relations for Rhesus monkey kidney tissue, experimental and theoretical results.
a) loading speed 5 cm/s, corresponding to the strain rate of about 0.385 s^{-1},
b) loading speed 250 cm/s, corresponding to the strain rate of about 19.24 s^{-1},
c) loading speed 500 cm/s, corresponding to the strain rate of about 38.47 s^{-1}.

and 5). The loading velocities were 5 cm/s, 250 cm/s and 500 cm/s which corresponded to the strain rates of approximately 0.225 1/s, 11.25 1/s and 22.5 1/s for the liver, and 0.385 1/s, 19.24 1/s, 38.47 1/s for the kidney. Larger strain rates for the kidney are the consequence of smaller dimensions of this organ. Melvin's result should be understood as average across the organs, since the tests were performed on the organs *in vivo* , not on tissue samples extracted from the specific locations.

As for the brain, the stress-strain curves are concave upward for all compression rates containing no linear portion from which a meaningful elastic modulus could be determined. The tissue response stiffened with the increasing loading speed, indicating a strong stress-strain rate dependence. The results shown in Figures 4 and 5 are in general agreement with those published in [28]. For slower strain rates there is no other data available for comparisons.

MATHEMATICAL MODELLING OF SOFT TISSUE MECHANICAL PROPERTIES

Soft tissue as a biphasic mixture

The biphasic theory (see e.g. [36,37]) assumes the tissue to be a mixture of two immiscible constituents: a solid deformable porous matrix and a penetrating fluid. The governing equations of biphasic continuum, are:

- Equation of continuity,
- Condition of saturation of the mixture, and
- Equation of equilibrium.

Additionally it is assumed that the fluid is inviscid and that the diffusive momentum exchange is proportional to the relative velocity between phases.

The accepted way to relate the stresses to the deformation (in a solid matrix) is by means of the Helmholtz free energy (similar to the strain energy – stresses depend on the current state of deformation only). The mathematical details can be found e.g. in [38].

The major assumption in the constitutive modelling of the mixture, is that the solid phase stress depends only on the current deformation and that the fluid is inviscid. Therefore, there is no energy dissipation in the system other than that coming from interactions between phases. The model states that this dissipation is proportional to the relative velocity between phases. What about loading conditions under which the relative velocity is very small? Let us consider the unconfined compression of soft tissue. Under unconfined conditions the sample, when being compressed, can expand laterally. Both phases are moving in a similar way, so

that the relative velocity of the phases is close to zero, therefore the dependence on loading velocity can not be reflected in the model. In fact, it was shown analytically [39] for the linear biphasic model and confirmed numerically for the non-linear case [40] that the ratio of the instantaneous stress (after sudden movement of the upper platen) to the equilibrium stress (after sufficiently long time following load application), as predicted by the biphasic theory, *cannot be larger than*

$$\frac{3}{2(1+\nu)} \in \langle 1,\ 1.5\rangle$$

where ν is the Poisson's ratio of the solid phase (or its finite deformation equivalent). This poses a severe limit on the stress dependence on loading velocity, which is in obvious conflict with experimental results. As apparent in Figure 3 Lagrange stresses in swine brain tissue for the compressive strain rate of 0.64 s^{-1} are more than six times larger than that for the compressive strain rate of 0.64×10^{-5} s^{-1}. Similarly (Figures 4 and 5), stresses in liver and kidney change much more with the increase in loading speed than the biphasic model can predict. The unconfined compression experiment results prove that the tissue's solid phase is inherently dissipative and the assumption of its hyperelasticity, should be abandoned.

Tissue as a viscoelastic single–phase continuum

As shown in Section 2, soft tissues exhibit non-linear stress-strain and stress-strain rate (loading velocity) mechanical behaviour. These two non-linear phenomena will be modelled separately.

Modelling of finite deformation non-linear tissue behaviour

The accepted way of mathematical modelling of isotropic, almost incompressible continua is based on choosing an appropriate form of the strain energy function. For soft tissues we propose the energy function in polynomial form successfully used before for certain types of incompressible rubbers [41]:

$$W = \sum_{i+j=1}^{N} C_{ij}(J_1-3)^i\,(J_2-3)^j \qquad (1)$$

Where J_1 and J_2 are so called strain invariants (see e.g. [42] for introduction to non-linear elasticity).

The energy dependence on strain invariants only comes from the assumption that the tissue is initially *isotropic*. The first two terms in (1) form a well known Mooney–Rivlin energy function, originally developed for incompressible rubbers (for discussion see [43]).

In experiments conducted the deformation was close to orthogonal. In such case computation of the only non–zero Lagrange stress components (measured with respect to undeformed configuration) is very simple:

$$T_{zz} = \frac{\partial W}{\partial \lambda_z} \qquad (2)$$

where l_z is a stretch in vertical direction.

Modelling of the loading velocity dependent tissue behaviour

To model the loading speed dependent behaviour of the tissue the coefficients in the formula for energy function (1) can be written in the form of exponential, time dependent series:

$$C_{ij} = C_{ij0}\left(1-\sum^{n} g_k\left(1-e^{-\frac{t}{\tau_k}}\right)\right) \qquad (3)$$

and the energy function can be presented in the form of a convolution integral:

$$W = \int^{t} \{\sum_{i+j=1}^{N}[C_{ij0}(1-\sum_{k=1}^{n} g_k(1-e^{-\frac{t-\tau}{\tau_k}}))]\frac{d}{d\tau}[(J_1-3)^i(J_2-3)^j]\}d\tau \qquad (4)$$

Substitution to (2) yields:

$$T_{zz} = \int^{t} \{\sum_{i+j=1}^{N}[C_{ij0}(1-\sum_{k=1}^{n} g_k(1-e^{-\frac{t-\tau}{\tau_k}}))]\frac{d}{d\tau}[\frac{\partial}{\partial\lambda_z}((J_1-3)^i(J_2-3)^j)]\}d\tau \qquad (5)$$

Equation (5) served as a basis for the comparison of the theory and experiment. Mechanical parameters requiring identification are: C_{ij0} – describing the instantaneous elasticity of the tissue, t_k – characteristic times, and g_k – relaxation coefficients, k=1,..., n. N is the order of polynomial in strain invariants. For infinitesimal strain conditions, the sum of constants C_{100} and C_{010} has a physical meaning of one half of the instantaneous shear modulus, i.e.:

$$\frac{\mu_0}{2} = C_{100} + C_{010} \qquad (6)$$

Determination of material constants for swine brain tissue

For the determination of material coefficients in the model, the experimental results for the loading

phase of the unconfined compression of swine brain described in Section 2 were used. To obtain a good agreement between the theory and experiment, it was necessary to retain second order terms in the energy function (1). Then, for N=2:

$$T_{zz} = \int_0^t \{(1-\sum_{k=1}^{n} g_k(1-e^{-\frac{t}{\tau_k}}))*[C_{100}\frac{d}{d\tau}(2\lambda_z - 2\lambda_z^{-2}) + C_{010}\frac{d}{d\tau}(-2\lambda_z^{-3}) + C_{110}\frac{d}{d\tau}[(\lambda_z^2 + 2\lambda_z^{-1} - 3)(\lambda_z^{-2} + 2\lambda_z - 3)] + C_{200}\frac{d}{d\tau}[(\lambda_z^2 + 2\lambda_z^{-1} - 3)(2\lambda_z - 2\lambda_z^{-2})] + C_{020}\frac{d}{d\tau}[(\lambda_z^{-2} + 2\lambda_z - 3)(-2\lambda_z^{-3})]]\}d\tau \quad (7)$$

In the case of the compression with constant velocity, the integral (7) can be evaluated analytically, however, the result is long and not presented here. It is important to note that after fixing the values of parameters gk the expression for stress is linear in material parameters C_{ij0}. Similarly, after fixing constants C_{ij0} the model becomes linear in parameters g_k. This important property was used to estimate the values of material constants for swine brain tissue.

Two time–dependent terms (n=2 in eg. 7) were used. This was a minimal number of exponentially decaying terms allowing for accurate modelling the tissue behaviour for a wide range of loading velocities. It proved not possible with only one exponentially decaying time dependent term to reproduce the experimental results for strain rates ranging over five orders of magnitude. To uniquely determine material coefficients C_{ij0} and g_k (eq. 7) a few additional assumptions were adopted. The equality of the energy of reciprocal deformation to that of the original one (see [44]) was assumed:

$$\frac{C_{01}}{C_{10}} = 1 \text{ and } \frac{C_{02}}{C_{20}} = 1 \bullet C_{110}$$

was assumed to be equal 0. Two time constants, t_1= 5 [s]; t_2=50 [s], were chosen to be approximately equal to the duration of the medium and fast tests respectively. These assumptions left four constants to be determined: C_{100}, C_{200}, g_1 and g_2.

A simple iterative procedure was used to uniquely determine the required four parameters. Maximum likelihood method was employed to obtain the best set of material coefficients to describe the experimental data. The estimated material properties of swine brain at low strain rates are listed in Table 1. Figure 3 presents the comparison of experimental results and theoretical prediction of the linear viscoelastic model.

The agreement for fast and medium loading speeds is very good (Figure 3 a,b). Worse match for slow loading speed results from a different character of the stress-strain curve than that for medium and fast loading speeds. In the hyperelastic, linear viscoelastic model the shape of stress – strain curve does not depend on strain rate (see Figure 3).

Determination of material constants for liver and kidney

The results of [33] were used for liver and kidney model identification. To accurately account for the tissue behaviour for our range of loading velocities, it was sufficient to use only one time–dependent term in the C_{ij} expansion (n=1 in eg. 3). To uniquely determine material coefficients C_{ij0} and g_k the same additional assumptions as for the brain were adopted. The time constants, t_1=0.002 [s], was chosen basing on the duration of the loading phase in experiments and the considerations for the brain [19].

As for the brain, the maximum likelihood method was used to identify the material parameters. Table 2 contains the values of estimated material coefficients for liver tissue together with multiple correlation coefficients characterising the quality of fit. Corresponding values for the kidney are presented in Table 3. Figures 4 and 5 present the comparison of experimental results and theoretical predictions of the linear viscoelastic model.

It is worth noting that the instantaneous shear moduli for liver and kidney are very close to each other.

Table 1. Brain material coefficients and multiple correlation coefficients

Instantaneous response	characteristic time t_1=0.5 [s]	characteristic time t_2=50[s]
C_{100}= C_{010}=263 [Pa];	g_1=0.450;	g_2=0.365;
C_{200}= C_{020}=491 [Pa];	R^2=0.986	R^2=0.986
μ_0=2(C_{100}+ C_{010})=1052[Pa]		
R^2=0.996		

Table 2. Liver material coefficients and multiple correlation coefficients.

Instantaneous response	characteristic time t_1=0.002 [s]
C_{100}= C_{010}=63619 [Pa];	g_1=0.9;
C_{200}= C_{020}=13222 [Pa];	R^2=0.974
μ_0=2(C_{100}+ C_{010})=254476 [Pa]	
R^2=0.996	

Table 3. Kidney material coefficients and multiple correlation coefficients.

Instantaneous response	characteristic time t_1=0.002 [s]
C_{100}= C_{010}=64176 [Pa];	g_1=0.94;
C_{200}= C_{020}=92030 [Pa];	R^2=0.983
μ_0=2(C_{100}+ C_{010})=256704 [Pa]	
R^2=0.9975	

DISCUSSION AND CONCLUSIONS

In this study a simple, linear viscoelastic model of tissue deformation behaviour is presented. The model accounts well for observed non-linear stress-strain relations, as well as for strong dependence between stresses and strain rate.

The use of the single-phase, linear, viscoelastic model based on the concept of the strain energy function, in the form of convolution integral with coefficient expressed in the form of exponential series, is described. The model requires, in the case of brain, four, and in the cases of liver and kidney only two material constants to be identified. The main advantage, though, is that the large deformation, linear viscoelastic model can be immediately applied to larger scale finite element computations [45] by directly using ABAQUS commands HYPERELASTIC – to describe instantaneous elasticity of the tissue, and VISCOELASTIC – to account for time dependent tissue behaviour [46].

Characteristic times used in this study are considerably larger than those used in hypergravity, impact and injury modelling. The tissue stiffness resulting from analysis of typical for surgical procedures, slow strain rate experiments, is much lower than that assumed in models intended to explain high strain rate phenomena. Therefore one must be very cautious in choosing the appropriate model for one's anticipated strain rate range. The instantaneous brain stiffness governed by constants C_{100}=263Pa and C_{200}=491Pa (equivalent to the instantaneous shear modulus m_0=1052Pa) will not, obviously, be adequate for describing tissue behaviour at strain rates larger than 0.7 1/s.

It is well known that changes in impact velocity greatly affect the injury level [25,31]. The inclusion of the stress – strain rate dependence in the constitutive model provides means to model such behaviour.

The mathematical models presented here are useful in approximate modelling the behaviour of abdominal organ tissues. The presented approach employs spatial averaging of material properties. The strain rate range investigated ascertains that the model is meaningful in car crash or other situations leading to impacts at high speeds. Similar procedure can lead to constructing a constitutive model for applications in surgical simulations. However, the experimental results concerning the deformation behaviour of abdominal organs at low strain rates (say 0.01 1/s, typical for neurosurgery) are not available yet.

Before the finite element simulation of liver and kidney deformation is conducted, further research is needed to determine the way these organs are attached to the body. Such knowledge is necessary to formulate properly the boundary conditions for the mathematical formulation of the problem.

An alternative way of modelling brain tissue seems to be a biphasic approach. However, as it was shown in Section 3, biphasic models in their present form can not account for strong stress – strain rate dependence observed in the brain tissue.

Acknowledgments

The financial support of the Australian Research Council and Japanese Science and Technology Agency is gratefully acknowledged.

REFERENCES:

1. *Borowski S, Dietrich M, Kedzior K et al: Modeling and Simulation of Human Musculoskeletal System. In Proceedings of the Sixth Biomechanics Seminar (Edited by Hogfors C and Andreasson G), Center for Biomechanics, Chalmers University of Technology, Sweden, 1992; 116-134*
2. *Fung YC: Biomechanics. Mechanical properties of Living Tissues. Springer-Verlag, New York, 1981*
3. *Gallagher RH, Simon BR, Johnson PC and Gross JF eds: Finite Elements in Biomechanics. John Wiley & Sons. New York, 1982*
4. *Mow VC, Ateshian GA and Spilker RL: Biomechanics of Diarthrodial Joints: A Review of Twenty Years of Progress. Trans. ASME, J Biomech Eng, 1993; 115: 460-467*
5. *Schmid-Schonbein GW, Woo SL-Y and Zweifach BW eds: Frontiers in Biomechanics. Springer, New York, 1986*
6. *Brett PN, Fraser CA, Henningan M et al: Automatic Surgical Tools for Penetrating Flexible Tissues. IEEE Eng Med Biol, 1995; May/June: 264-270*
7. *Burdea G: Force and Touch feedback for Virtual Reality. Wiley. New York, 1996*

8. *Miller K and Chinzei K: Modeling of Soft Tissues, Mechanical Engineering Laboratory News, 1995; 12: 5-7 (in Japanese)*
9. *Miller K and Chinzei K: Modeling of Soft Tissues Deformation, Journal Computer Aided Surgery, 1, Supl, Proc. of Second International Symposium on Computer Aided Surgery, Tokyo Women's Medical College, Shinjuku, Tokyo, 1995; 62-63*
10. *Lavallée S: Registration for Computer Integrated Surgery: Methodology, State of the Art. Computer-Integrated Surgery, MIT Press, Cambridge Massachusetts, 1995; 77-97*
11. *Huelke DF and Melvin JW: Anatomy, Injury Frequency, Biomechanics, and Human Tolerances. SAE Transactions 800098, 1980; 633-651*
12. *Ommaya AK: Mechanical Properties of Tissues of the Nervous System. J Biomech, 1968; 1: 127-138*
13. *Walsh EK and Schettini A: Calculation of brain elastic parameters in vivo. Am J Physiol, 1984; 247: R637-R700*
14. *Sahay KB, Mehrotra R, Sachdeva U and Banerji AK: Elastomechanical Characterization of Brain Tissues. J Biomech, 1992; 25: 319-326*
15. *Estes MS and McElhaney JH: Response of Brain Tissue of Compressive Loading, ASME Paper No. 1970; 70-BHF-13*
16. *Galford JE and McElhaney JH: A Viscoelastic Study of Scalp, Brain and Dura. J Biomech, 1970; 3: 211-221*
17. *Voo L, Kumaresan S, Pintar FA et al: Finite-element models of the human head. Med Biol Eng Comp, 1996; 34: 375-381*
18. *Pamidi MR and Advani SH: Nonlinear Constitutive Relations for Human Brain Tissue. Trans ASME, J Biomech Eng, 1978; 100: 44-48*
19. *Mendis KK, Stalnaker RL and Advani SH: A Constitutive Relationship for Large Deformation Finite Element Modeling of Brain Tissue. Trans. ASME, J Biomech Eng, 1995; 117: 279-285*
20. *Guillaume A, Osmont D, Gaffie D et al: Effects of Perfusion on the Mechanical Behavior of the Brain Exposed to Hypergravity. J Biomech, 1997; 30(No. 4): 383-389*
21. *Donnelly BR and Medige J: Shear Properties of Human Brain Tissue. J Biomech Eng, 1997; 119: 423-432*
22. *Divicenti FC, Rives JD, Laborde EJ et al: Blunt Abdominal Trauma, J Trauma, 1968; 8(6): 1004-1013*
23. *Guerriero G: Traumatic injury to the kidney and ureter, Current Opinion in Urology, 1993; 3: 186-193*
24. *Hossak DW: The Pattern of Injuries Received by 500 Drivers and Passengers Killed in Road Accidents, Medical Journal of Australia, 1972; 2: 193-195*
25. *Rouhana SW, Lau IV and Ridella SA: Influence of Velocity and Forced Compression on the Severity of Abdominal Injury in Blunt, Nonpenetrating Lateral Impact, J Trauma, 1985; 25: 490-500*
26. *Rutledge R, Thomason M, Oller D et al: The Spectrum of Abdominal Injuries Associated with the Use of Seat Belts, J Trauma, 1991; 31: 820-826*
27. *Yamada H: Strength of Biological Materials, The Wiliams & Wilkins Company, 1970*
28. *Farshad M, Barbezat M, Schmidlin F et al: Material Characterization and Mathematical Modelling of the Pig Kidney in Relation with Biomechanical Analysis of Renal Trauma, Proceedings of North American Congress on Biomechanics. Waterloo, Ontario, Canada, 1998*
29. *Schmidlin FR, Schmid P, Kurtyka T et al: Force transmission and stress distribution in a computer simulated model of the kidney: an analysis of the injury mechanisms in renal trauma, J Trauma, 1996; 40: 791-796*
30. *Viano DC, King AI, Melvin JW and Weber K: Injury Biomechanics Research: An Essential Element in the Prevention of Trauma, J Biomech, 1989; 22(5): 403-417*
31. *Viano DC and Lau IV: A Viscous Tolerance Criterion for Soft Tissue Injury Assessment, J Biomech, 1988; 21(5): 387-399*
32. *Viano DC, Lau IV and Asbury C: Biomechanics of the Human Chest, Abdomen, and Pelvis in Lateral Impact, Accid Anal & Prev, 1989; 21(6): 553-574*
33. *Melvin JW, Stalnaker RL and Roberts VL: Impact Injury Mechanisms in Abdominal Organs, SAE Transactions, 1973; 730968: 115-126*
34. *Kumagaya T and Namioka S (eds): 'Hyology and Hyoiatrics, ' Kindai Press, Tokyo, 1987 (in Japanese)*
35. *Ruan JS, Khalil T and King AI: Dynamic Response of the Human Head to Impact by Three-Dimensional Finite Element Analysis. Trans. ASME, J Biomech Eng, 1994; 116: 44 -50*
36. *Nagashima T, Horowitz B, Rapoport SI: A Mathematical Model of Vasogenic Brain Edema, Advances in Neurosurgery, 1990; 52: 317-325*
37. *Almeida and RL Spilker: Mixed and Penalty Finite Element Models for the Nonlinear Behaviour of Biphasic Soft Tissues in Finite Deformation, Comp Meth Biomech Biomed Eng, 1997; 1: 25-46*
38. *Mow VC, Kuei SC, Lai WM and Armstrong CG: Biphasic Creep and Stress Relaxation of Articular Cartilage in Compression: Theory and Experiments, Trans. ASME, J Biomech Eng, 1980; 102: 73-84*
39. *Armstrong CG, Lai WM and Mow VC: An Analysis of the Unconfined Compression of Articular Cartilage, Trans. ASME, J Biomech Eng, 1984; 106: 165-173*
40. *Miller K: Modelling Soft Tissue Using Biphasic Theory - A Word of Caution. Comp Meth Biomech Biomed Eng, 1998; 1: 261-263*
41. *Treloar LRG: The Physics of Rubber Elasticity. Calderon Press. Oxford. UK, 1975*
42. *Green AE and Zerna W: Theoretical Elasticity. Calderon Press. Oxford. UK, 1954*
43. *Rivlin RS: Forty Years of Nonlinear Continuum Mechanics. In Proceedings of the IX Int. Congress on Rheology, Mexico, 1984; 1-29*
44. *Mooney M: A Theory of Large Elastic Deformation. J Appl Phys, 1940; 11: 582-592*
45. *Zienkiewicz OC and Taylor RL: The finite element method: McGraw-Hill, London, New York, 1989*
46. *ABAQUS Theory Manual (1992) Version 5. 2, Hibbit, Karlsson & Sorensen, Inc*